Isospin correlations in isotope yields at intermediate and high energy heavy-ion collisions

Riza Ogul

Department of Physics, Faculty of Science, Selçuk University, 42079 Konya, Turkiye

In collaboration with: A.S. Botvina, W. Trautmann, Konya group, and many other colleagues

EFB25 European Conferences on Few-Body Problems in Physics
30 July-04 August 2023, Mainz

Symmetry Energy in Nuclear Dynamics

The experiments performed at advanced research centers GSI-FAIR, JINR, GANIL, CATANIA, MSU, TAMU, RIKEN, etc. have been used to investigate the properties of rare isotopes, nuclear structure, astrophysical events, nuclear dynamics from low to relativistic energies, fundamental interactions, and so on.

In nature, these reactions would take place in stars and exploding stellar environments such as novae and supernovae. EOS (symmetry energy) of nuclear matter is crucial in simulation of astrophysical events such as core-collapse supernovae and neutron stars.

Excitation energy stored in projectile or target sources:
Ex $\leq$ 1 MeV/nucleon, collective ossilations of compound nucleus observed.
Ex=1-2 MeV/nucleon, number of fragments=2, fission channels are superior.
Ex>2 MeV/nucleon, if the number of fragments with Z>2 is greater than 2, nuclear multifragmentation is pronounced.

Influence of the Symmetry Energy on Fragment Partitions

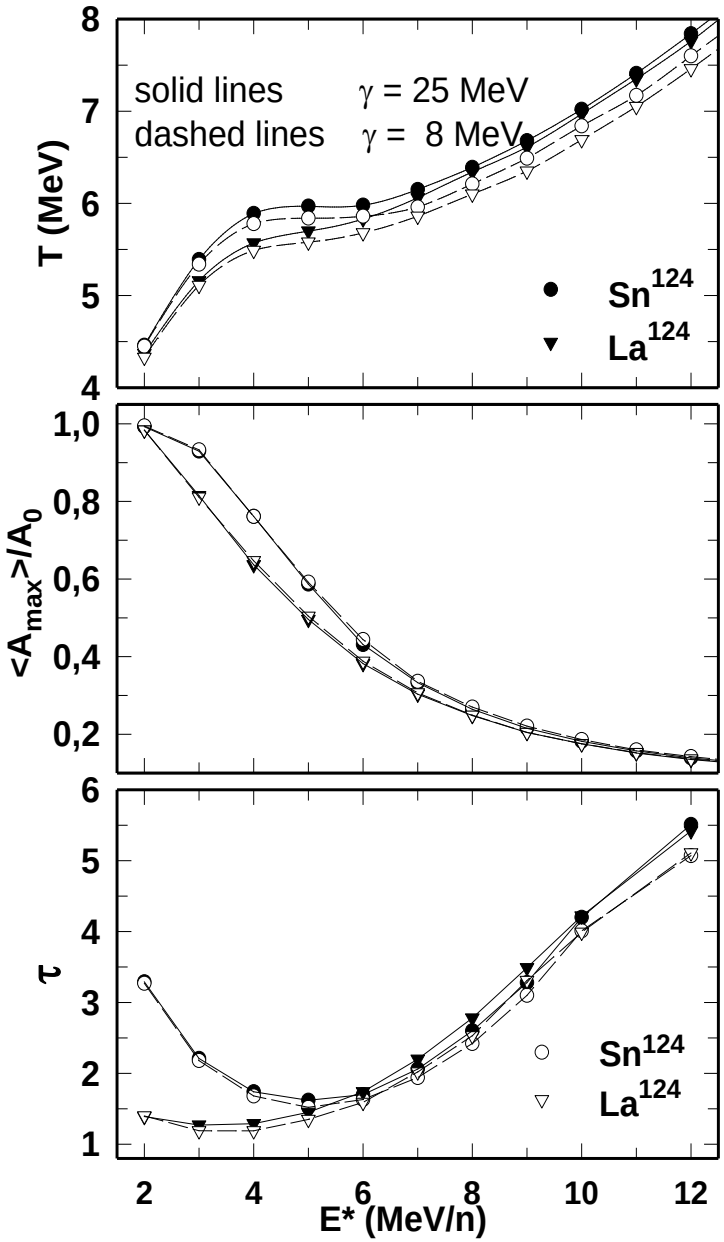

$$F_{AZ}^{sym} = \gamma\,(N-Z)^2 / A$$

The calculations for γ =25 MeV corresponding to the mass formula of cold nuclei and for γ =8 MeV for Sn^{124} (N/Z=1.480) and La^{124} (N/Z=1.175).

The caloric curve, Amax the mean maximum mass of fragments in partitions, and power-law parameters τ for different assumptions on the symmetry energy.

The results for γ =8 MeV are only slightly different from those obtained for the standard value γ =25 MeV.

One can see a small decrease of T, therefore, the average characteristics of produced hot fragments are not very sensitive to the symmetry energy. The main effect of the symmetry energy is manifested in mass variances of the hot fragments (isotope distribution).

Influence of Symmetry Energy on Isotope Distribution

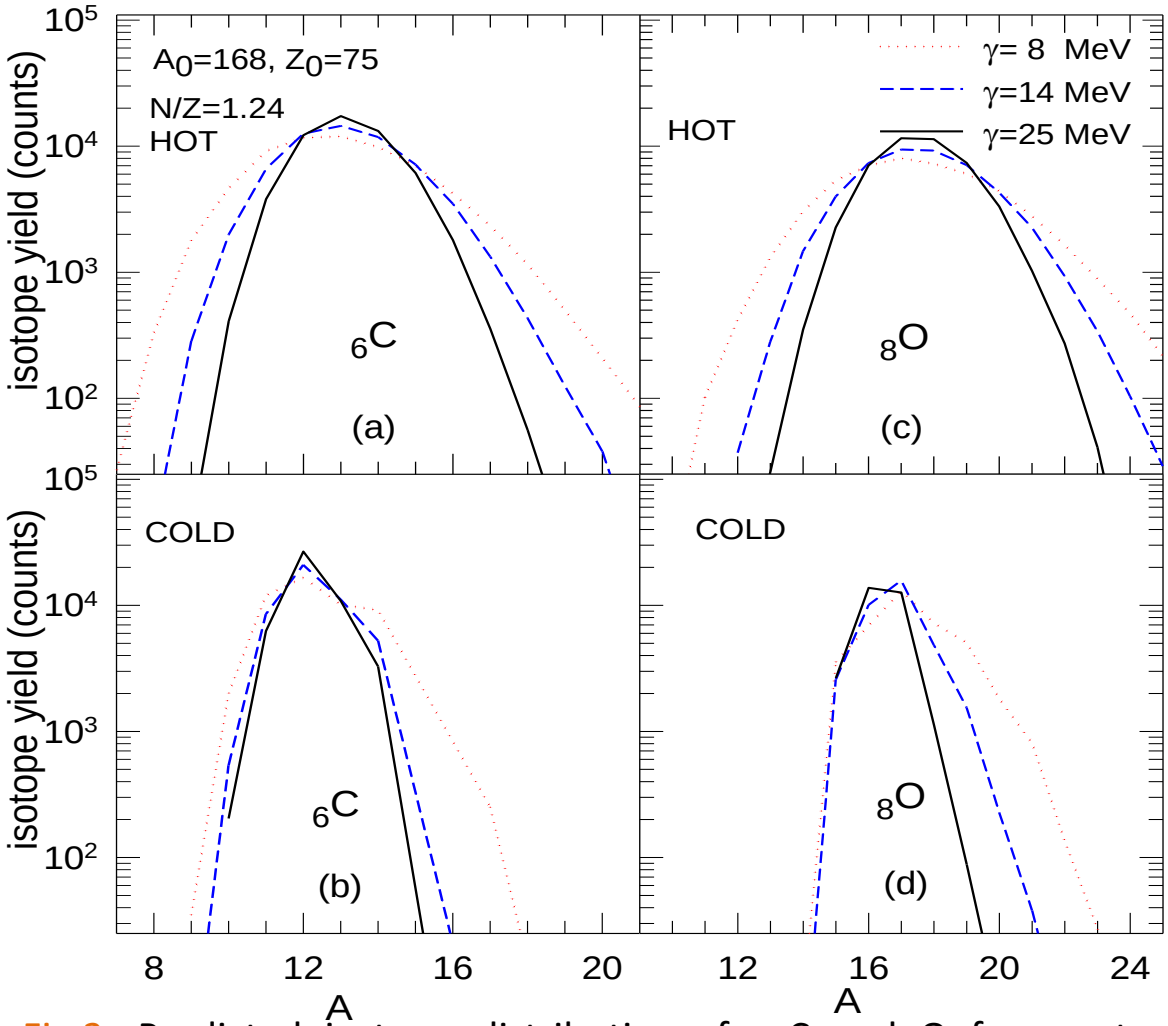

Fig.3: Predicted isotope distributions for C and O fragments emitted from the sources A_0=168, Z_0=75. The panels (a) and (c) show the primary hot fragments, and the panels (b) and (d) the secondary cold fragments of carbon and oxygen, respectively.

Influence of symmetry energy is significant which enable us to search for the values of symmetry energy at low density freeze-out.

For example: One can see the how isotope distribution curves widen with symmetry energy (MSU-exp. ^{112}Sn + ^{112}Sn central collision at 50 MeV/nucleon).

To search for the optimum reproduction of exp value of γ ?

The distribution of primary hot fragments becomes rather broad for γ=14 and 8 MeV. The primary fragments are supposed to decay by secondary evaporation of light particles or by the Fermi-break-up.

Production, Separation, Identification of Exotic Nuclei

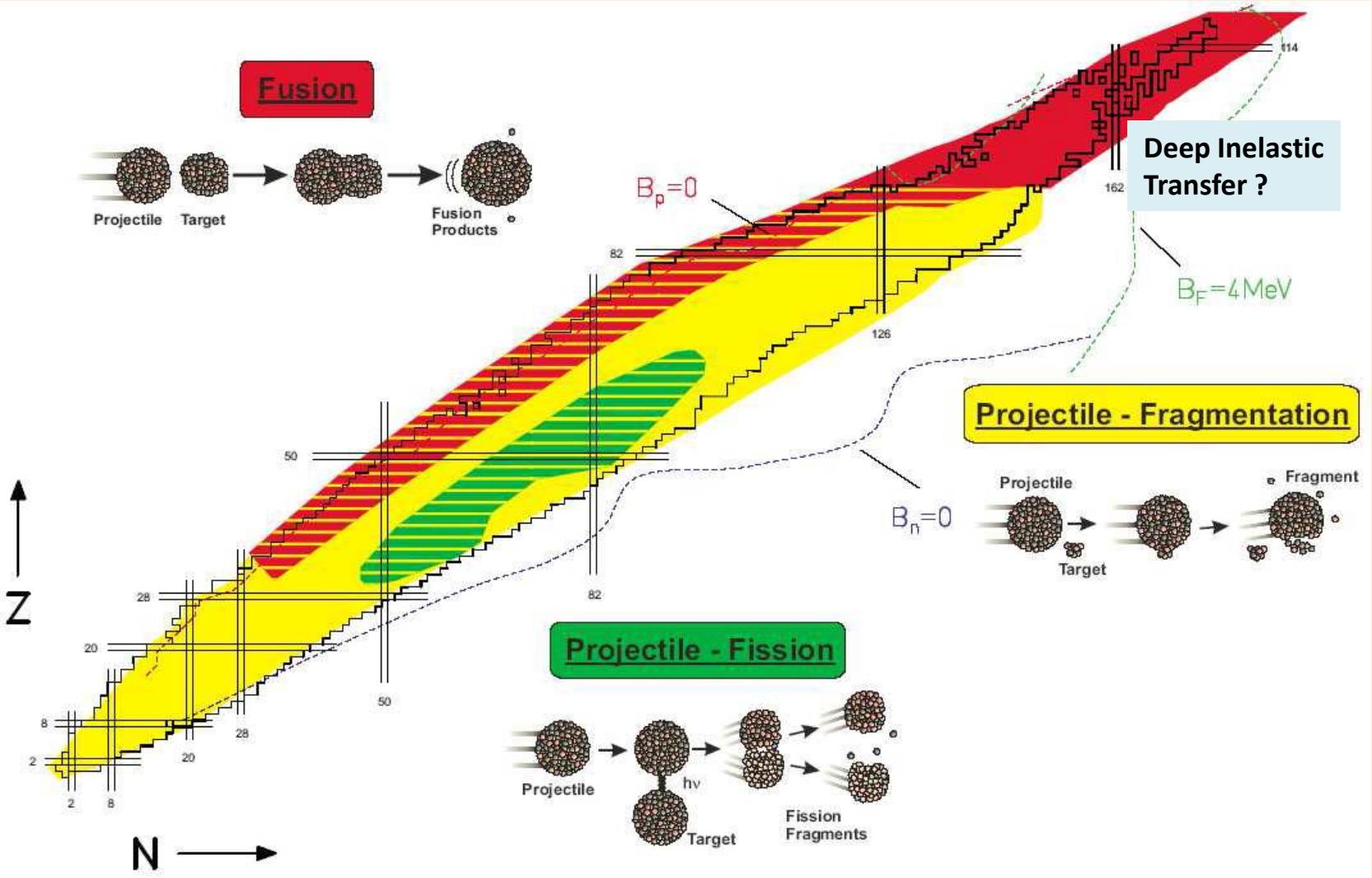

Nuclear Reactions and Separation of exotic nuclei: a) ISOL (Isotope Sep. On-Line) and b)In-Flight Separation-DIT products by velocity filter SHIP (in-flight separator) at GSI. New regions to be explored with NUSTAR at FAIR: next generation facility ! Storage Ring: for measurement of mass and lifetime of exotic nuclei.

Chart(S. Heinz): H. Geissel et al., Exotic Nuclear Beam Facilities, vol. 1. Wiley, 2014.

Outline

so far, thousands of radioactive isotopes are predicted to lie within the particle stability limits in nuclear chart, and around fifty per cent of them are identified.

There may be several elements occur in universe even though they cannot be found on earth, and some of them may be detectable in cosmic rays. Various research groups at the several accelerator facilities are trying to produce new elements/isotopes. In some laboratories including GSI, JINR, and RIKEN new elements in between Z = 107 (Bohrium-Bh) and Z = 118 (Oganesson-Og) were discovered in the period of the years 1981 and 2006.

They are mostly unstable and decay after a short time in milliseconds, therefore they are not directly observed, but their decay chains can be measured.

However, theoretical calculations have predicted the island of stability, whereby the isotopes of superheavy elements with Z > 103 might have considerably longer lifetime.

Experiments

ALADIN Experiments: E/A=600 MeV/A, projectiles Sn^{124} , Sn^{107} , La^{124} stable&radioactive secondary beams produced at FRS and measured at ALADIN-GSI at Schwerionen Synchrotron (SIS). ($Z \leq 10$ fragments).

FRagment Separator (FRS): E/A= 1 GeV/A, Sn^{124} + Sn^{124} and Sn^{112} + Sn^{112} measured with high-resolution magnetic spectrometer FRS. ($Z \leq 45$ fragments up to near-projectile fragments).

MSU Experiments: E/A= 50 MeV/A, $Sn^{112,124}$ beams on $Sn^{112,124}$ measured at National Superconducting Cyclotron of MSU ($Z \leq 10$ fragments).

FAZIA Experiments: E/A = 35 MeV/A, at Fermi energies, Kr^{80} beams on $Ca^{40,48}$ targets measured at at the Superconducting Cyclotron of the Laboratori Nazionali del Sud (LNS) of INFN (Catania).

Observables

The following observables are found to be sensitive to the variation of symmetry energy parameter γ.

One may search for the influence of the symmetry energy on fragment yields and density dependent values of γ for EOS of nuclear and stellar matter can be determined.

1. Isotope distributions
2. Average N/Z distributions
3. Isoscaling parameters

Statistical Approach to Multifragmentation

It is assumed in statistical multifragmentation model-SMM that a statistical equilibrium is reached in the low density freeze-out region.

The breakup channels are composed of nucleons and nucl. fragments, the laws of conservation of energy , momemtum, ang. momentum, A, and Z are considered.

The compound-nucleus channels such as evaporation and fission processes at low excitation energies ($E^* \leq 1$ MeV/nucleon, Weisskopf evaporation) as well as the transition region between the low- and the high-energy de excitation regimes are also included, and competition among all channels is permitted.

In the thermodyn. limit, SMM is consistent with liquid-gas phase transitions when the liquid phase is represented by infinite nuclear clusters [1], which allow connections for the astrophysical studies [2].

We calculate the statistical weights of all breakup channels . The decay channels are generated by the Monte Carlo method according to their statistical weights. In the Markov chain SMM we use the ingradients of standard SMM. Free energy of the fragments are parametrized as

$$F_{A,Z} = F_{A,Z}(\text{bulk}) + F_{A,Z}(\text{surface}) + F_{A,Z}(\text{coul.}) + F_{A,Z}(\text{symm.})$$

Statistical Approach to Multifragmentation [4]

probability of a given partition: $W_f^{mic} = \frac{1}{\xi}\exp\{S_f(E_0, A, Z)\}$, with $\xi = \sum_f \exp\{S_f(E_0, A, Z)\}$

mass and charge conservation: $\sum_{A,Z} N_{AZ}.A = A_0$, $\sum_{A,Z} N_{AZ}.Z = Z_0$

energy conservation: $E_0 = F_f - T_f \frac{\partial F_f}{\partial T_f}$

entropy of channel: $S_f = -\frac{\partial F_f}{\partial T_f}$

Fragments obey Boltzmann statistics, liquid-drop description of individual fragments, Coulomb interaction in the Wigner-Seitz approximation

free energy of channel: $F_f = \sum_{A,Z} N_{AZ} F_{AZ} + \frac{3}{5}\frac{Z_0^2 e^2}{r_0 A_0^{1/3}(1+\chi_c)^{1/3}}$

individual fragments: $F_{AZ} = F_{AZ}^b + F_{AZ}^s + F_{AZ}^{sym} + F_{AZ}^c$ $\quad W_0 = 16\ MeV$

bulk term: $F_{AZ}^b = [-W_0 - T_f^2/\varepsilon_0(A)]A,$ $\quad B_0 = 18\ \mathrm{MeV}$

surface term: $F_{AZ}^s = B_0[(T_c^2 - T_f^2)/(T_c^2 + T_f^2)]^{5/4} A^{2/3},$ $\quad T_c = 18\ \mathrm{MeV}$

symmetry term: $F_{AZ}^{sym} = \gamma(N - Z)^2 / A,$ $\quad \gamma = 25\,\mathrm{MeV}$

Coulomb term: $F_{AZ}^c = \frac{3}{5}\frac{Z_0^2 e^2}{r_0 A_0^{1/3}}[1 - (1+\chi_c)^{-1/3}],$

Statistical Ensemble Approach

In the ensemble approach, the multifragmentation process is subdivided into :

1. a dynamical stage leading to the formation of an equilibrated nuclear system,

2. formation of primary hot fragments, 3. deexcitation of the hot fragments are defined by statistical multifragmentation model.

For the description of the nonequilibrium stage of peripheral heavy-ion collisions, a variety of models can be used. Realistic calculations of ensembles of excited residual nuclei that undergo multifragmentation were first performed with the intranuclear cascade (INC) model [5]. More recent examples of hybrid calculations using INC or Boltzmann-Uehling-Uhlenbeck (BUU) models for the dynamical stage have been reported in Refs. [6,7].

Statistical Ensemble Approach

Experimentally established: 1) few stages of reactions leading to multifragmentation, 2) short time ~100fm/c for primary fragment production, 3) freeze-out density is around $0.1\rho_0$ -$0.4\rho_0$, 4) high degree of equilibration at the freeze-out.

formation of an equilibrated nucl. system --> disassembly of the system--> deexcitation

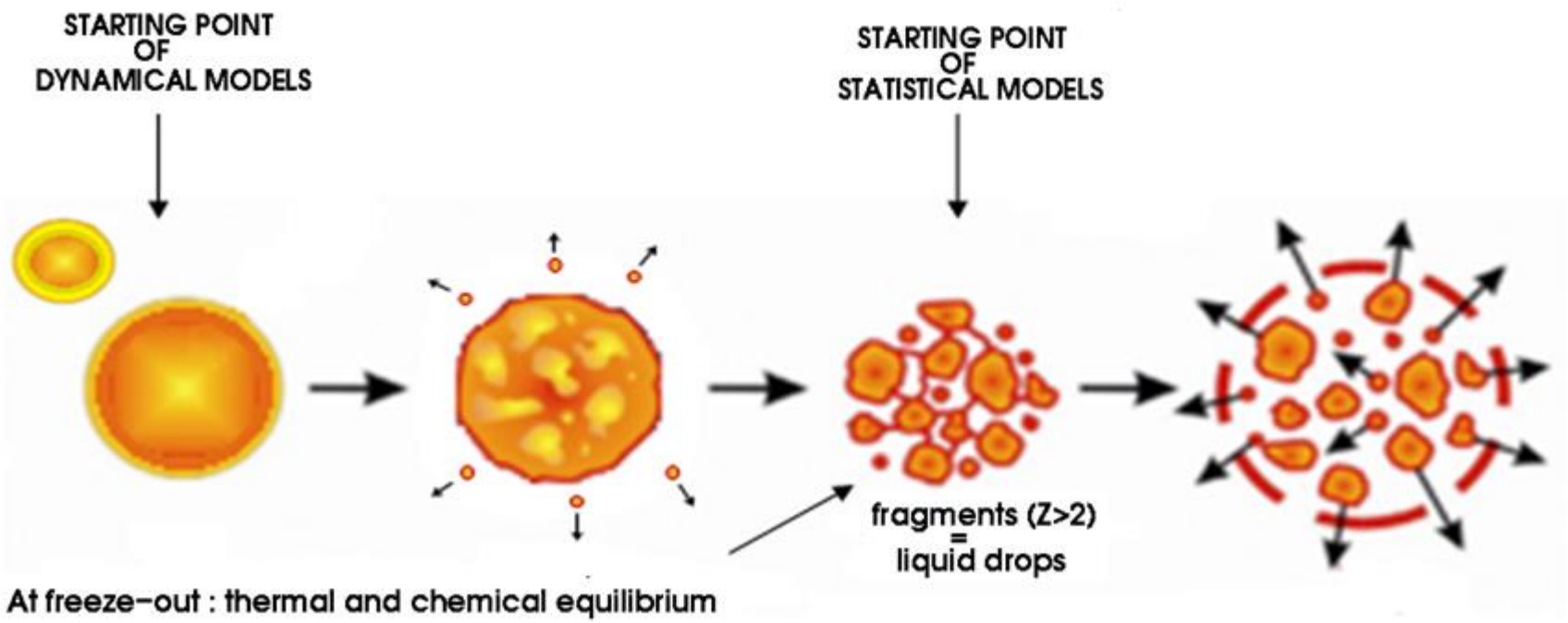

Parametrization of Ensemble of sources

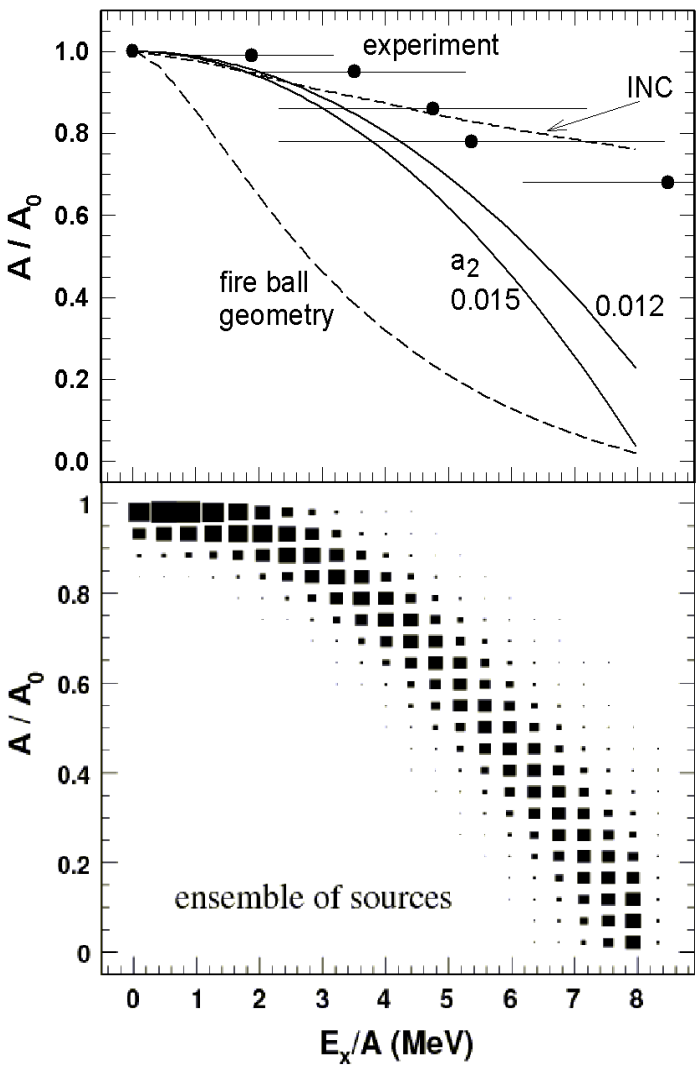

Fig.1. Top panel: Mean reduced mass number A/A_0 of relativistic projectile residuals as a function of their excitation energy Ex/A according to the fireball model of Gosset et al. [1], calculated for ^{107}Sn projectiles, and INC calculations for ^{197}Au + C [2] (dashed lines), according to the experimental results for ^{197}Au nuclei reported by Pochodzalla et al. [3] and including the widths in Ex/A (dots) and according to the parametrization used in this work for a_2 = 0.012 and 0.015 MeV^{-2} (solid lines). Bottom panel: Ensemble of hot thermal sources represented in a scatter plot of reduced mass number A/A0 versus excitation energy Ex/A, as used in the SMM calculations. The frequency of the individual sources is proportional to the area of the squares.

[1]. J. Gosset, et al., Phys. Rev. C 16, 629 (1977).
[2]. A. S. Botvina, et al.,Phys. At. Nucl. 57, 628 (1994).
[3]. J. Pochodzalla et al., Phys. Rev. Lett. 75, 1040 (1995).

Ensemble of sources- ALADIN & FRS exps.

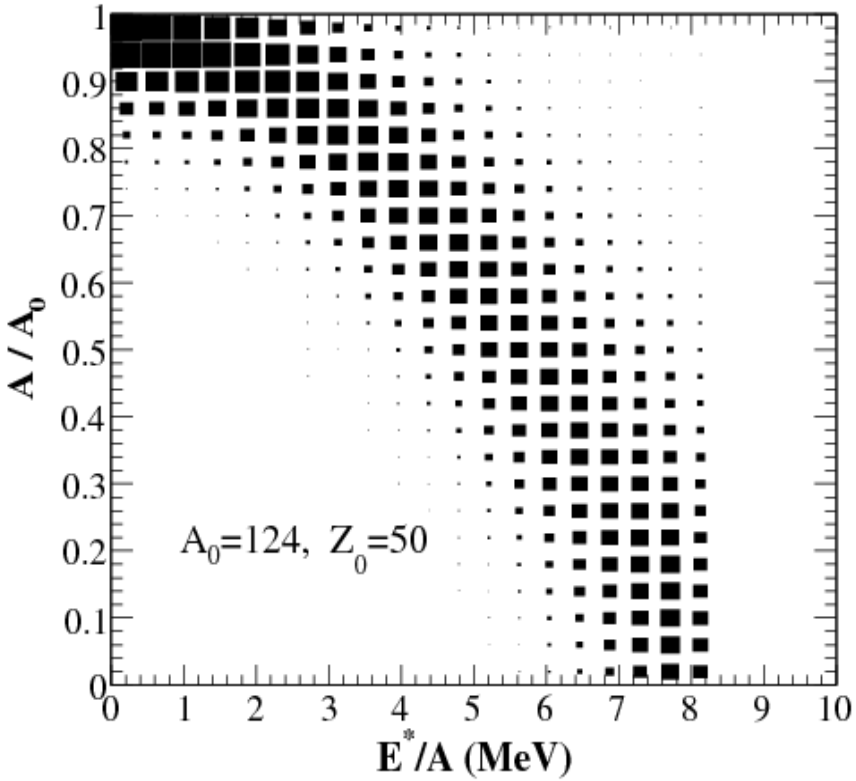

Fig.1. Ensemble of hot thermal sources represented in a scatter plot of reduced mass number A/A_0 of thermal sources as a function of their excitation energy E^*/A, as used in the SMM ensemble calculations. The intensity of the individual sources is proportional to the area of the squares.

The hot sources are formed according to the impact parameters. In this work, we follow Ref.[4]. which was rather effective in describing the multifrag of relativistic ^{197}Au projectiles, including their correlations and dispersions. The average masses of the equilibrated sources A were parametrized as

$$A/A_0 = 1 - a_1 (Ex/As) - a_2 (Ex/A_s)^2$$

where Ex is the excitation energy of the sources in MeV and A_0 is the projectile mass. According to the parametrization used in this work for $a_2 = 0.012$ and 0.015.

Ref. A. S. Botvina et al., Nucl. Phys. A 584, 737 (1995).

Relativistic Heavy-Ion Reactions: a) ALADIN Experiments

ELEMENT	A0	Z	N	N/Z
^{124}Sn	124	50	74	1.48
^{124}La	124	57	67	1.18
^{107}Sn	107	50	57	1.14

Table 1.The neutron content of the nuclei affects the fragment production in multifrag. of finite nuclei.

We consider 3 different sources Sn^{124} neutron-rich, and La^{124}, Sn^{107} neutron-poor to see how isospin effects the multifragmentation with their proton to neutron ratios (N/Z) are 1.48, and 1.18, 1.14, respectively. All beams had a laboratory energy of 600 MeV/nucleon on natSn . Isotopic composition of projectiles are expected fully preserved during the collision.

Isotopic yields for light particles ($Z \leq 10$) and IMF have been measured and calculated within SMM-ensemble by means of isoscaling, isotopic curves and N/Z to address open questions about modifications of symmetry and surface terms

[5]. R. Ogul, et al., *Phys. Rev. C* 83, 024608 (2011).

For the quantitative comparison of theory and experiment, the SMM ensemble calculations were globally normalized with respect to the measured Z_{bound} cross sections in the interval $10 \leq Z_{bound} \leq 30$ for which the agreement is best.

The corresponding distributions are obtained from ensemble calculations for 500000 reaction events. Parameters are determined by searching for an optimum reproduction of the measured fragment-charge distributions.

The obtained factors are 0.00937 mb, 0.00804 mb, and 0.0106 mb per theoretical event for ^{107}Sn, ^{124}Sn, and ^{124}La projectiles, respectively, i.e., on average about 100 events per mb were calculated with the SMM.

The agreement between theory and experiment is overall very satisfactory for charge and isotopic yields.

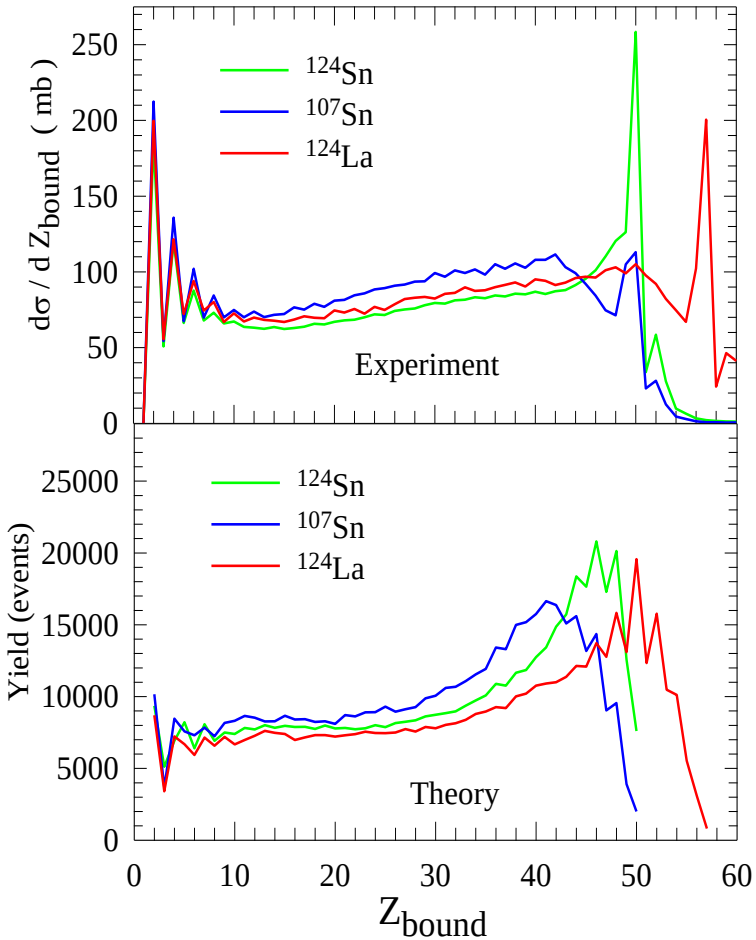

Fig.2. Top panel shows the triggered reaction cross section as a function of Zb for the three projectiles as indicated. Bottom panel shows the corresponding distributions as obtained from SMM ensemble calculations for 500 000 reaction events (100 event per mb).

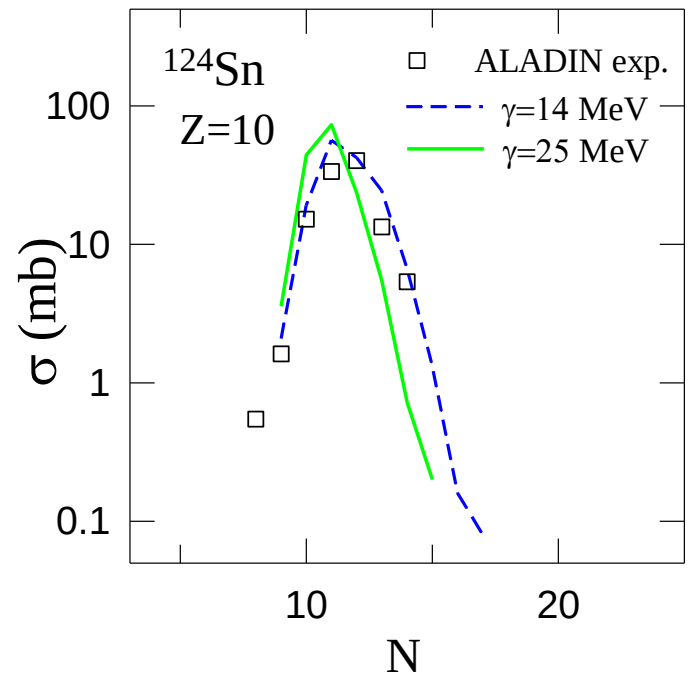

Fig.3. Isotope distribution for ^{124}Sn, empty squares show the ALADIN experimental data. SMM ensemble calculations were globally normalized to the measured Zbound cross sections in the interval $10 \leq Z_{bound} \leq 30$ for which agreement is the best (see Fig.2), the obtained normalization factor is 0.00804 mb per theoretical event for ^{124}Sn projectile.

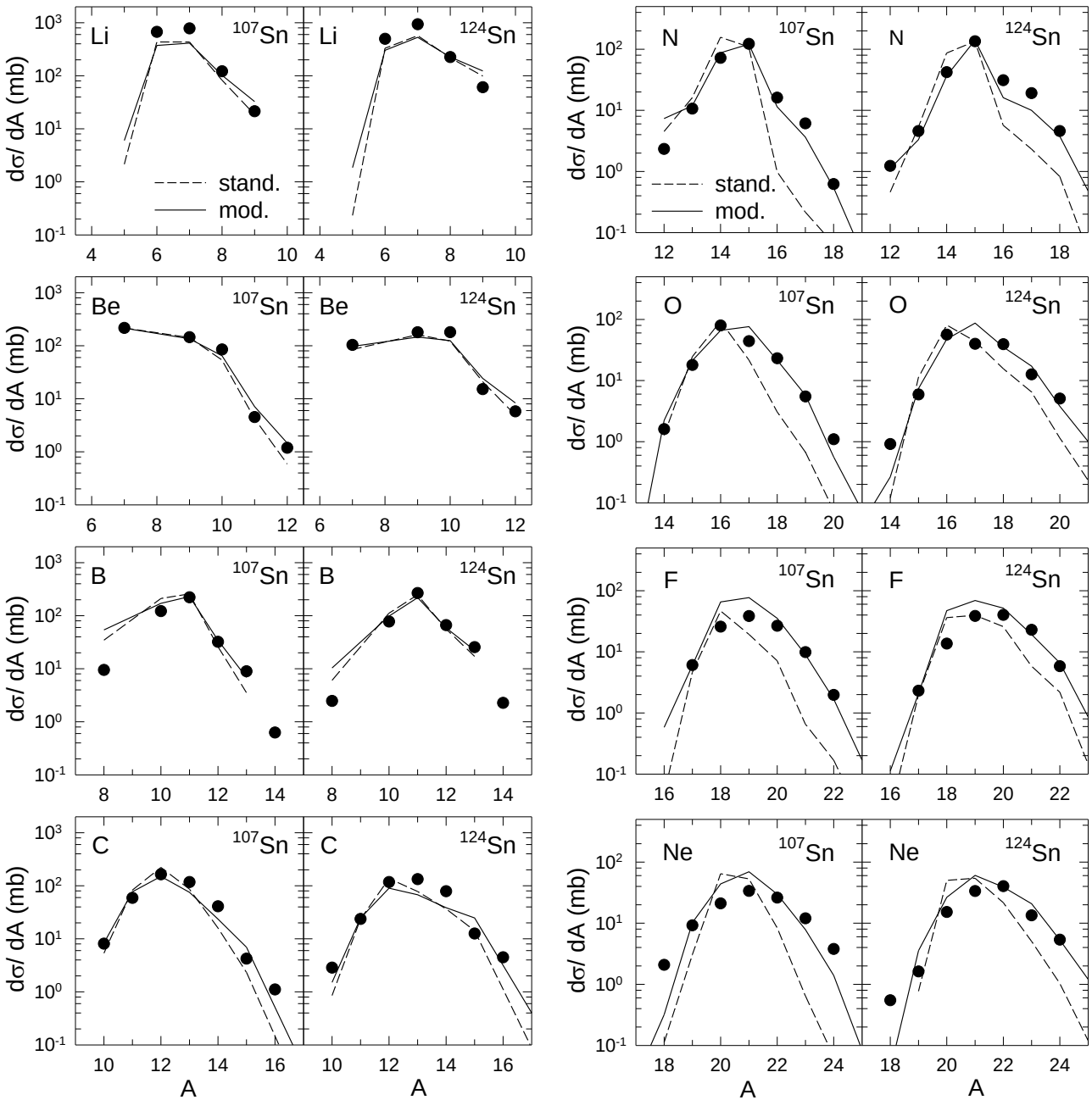

Fig.4. Isotopic distributionsfor light fragments in $3 \leq Z \leq 10$ with ensemble calculations for ALADIN data.

Experimental values are reproduced around γ =14 MeV shown by solid lines.

Average N/Z Calculations

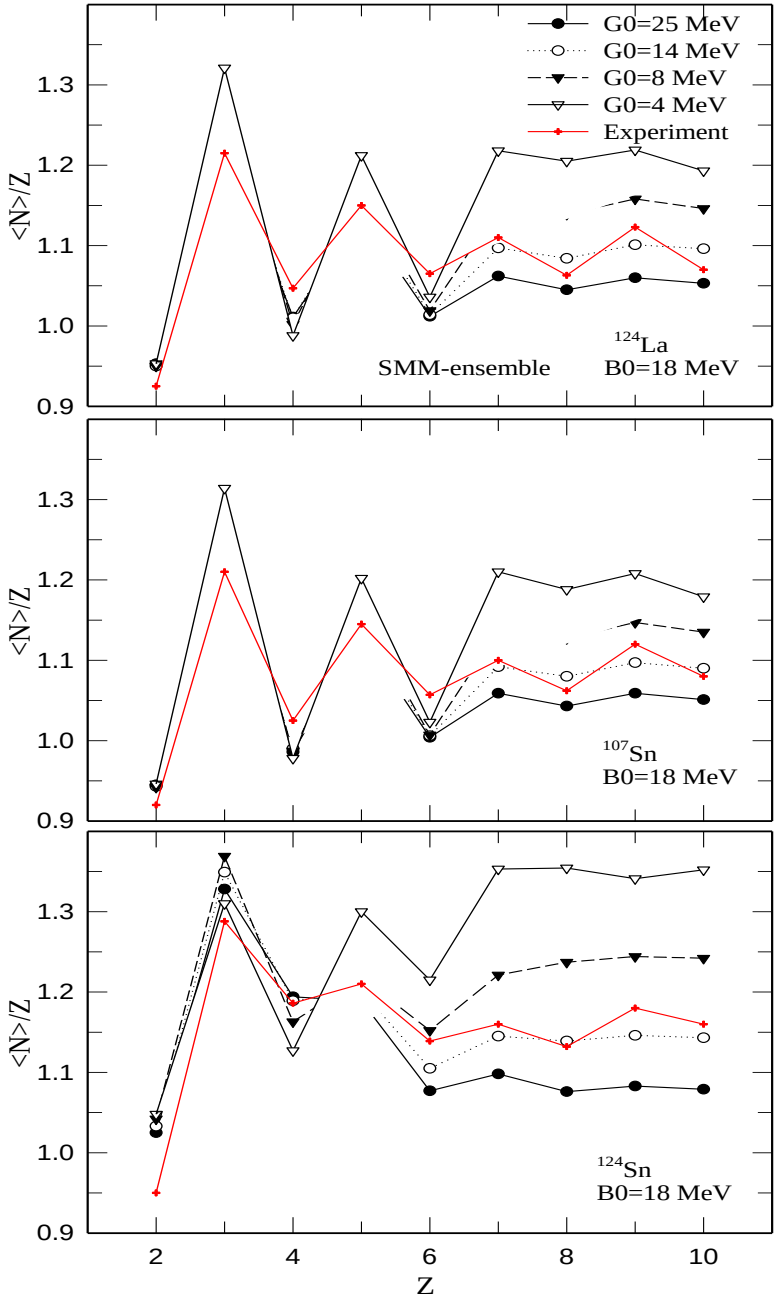

To reproduce the ALADIN data symmetry energy term is reduced to somewhere around γ = 14 MeV.

An overall good agreement at γ = 14 MeV is observed.

The odd-even staggering for (Z=5-10) and its relation to the composition of the source have been seen to be universal.

Fig.7. ALADIN-GSI data and ensemble calculations: variations of N/Z values with charge number Z of the fragments of the projectile multifragmentation. Red lines show experimental values, black lines show the modified values at various symmetr energy param γ.

Ref. R. Ogul, et al., *Phys. Rev. C* 83, 024608 (2011).

The Main Conclusion for ALADIN experiments

The agreement between theory and experiment is overall very satisfactory for charge and isotopic yields.

It is confirmed that a significant reduction of the symmetry term is found necessary to reproduce the data for light particles ($Z \leq 10$) by means of isotopic curves and N/Z analyses.

To reproduce the ALADIN data symmetry energy term is reduced to somewhere around $\gamma = 14$ MeV.

Nucleon-exchange at 600 MeV/nucleon is very unlikely. This is because Fermi spheres of projectile and target nuclei are well separated.

Relativistic Heavy-Ion Reactions: FRagment Separator (FRS)

Theoretical study of fragmentation products in the reactions:

^{112}Sn + ^{112}Sn and ^{124}Sn + ^{124}Sn at 1 A GeV.

FRS- experiment: The study of multifragmentation is extended to isotopic effects. To this goal, projectile fragmentation of two symetric systems ^{124}Sn + ^{124}Sn and ^{112}Sn + ^{112}Sn at an incident beam energy of 1 A GeV measured with high-resolution magnetic spectrometer FRS [1,2], and production cross sections of the projectile residues measured in these two reactions with Z= 10-46.

[1] V. Föhr, et al., Phys. Rev. **C 84**, (2011) 054605 (Exp Data)

[2] H. Imal, R. Ogul, et al., Phys. Rev. C **91**, 034605 (2015). (Theory)

FRagment Separator (FRS)-GSI

The experiment was performed at GSI to study influence of the isotopic composition of the projectile on the kinematical properties of projectile residues in peripheral and midperipheral relativistic heavy-ion collisions: N/Z = 1.24 for ^{112}Sn and 1.48 for ^{124}Sn

^{112}Sn + ^{112}Sn and ^{124}Sn +^{124}Sn

Projectile fragmentation of these two symetric systems is considered at an incident beam energy of 1 A GeV measured with high-resolution magnetic spectrometer Fragment Separator (FRS) [1].

The incident energy is chosen in such way to have the best conditions for the transmission of the reaction products through the FRS.

Beams were delivered from the universal linear accelerator (UNILAC) to the SIS18 heavy-ion synchrotron, where they were extracted and guided through the target area to the FRS [2].

Ref. [1]. V. Föhr, et al., Phys. Rev. **C 84**, (2011) 054605
Ref. [2]. H. Geissel et al., Nucl. Instrum. Methods Phys. Res., Sect. B **70,** 286 (1992).

Isotopic distributions of final fragments from Z=10 to Z=46

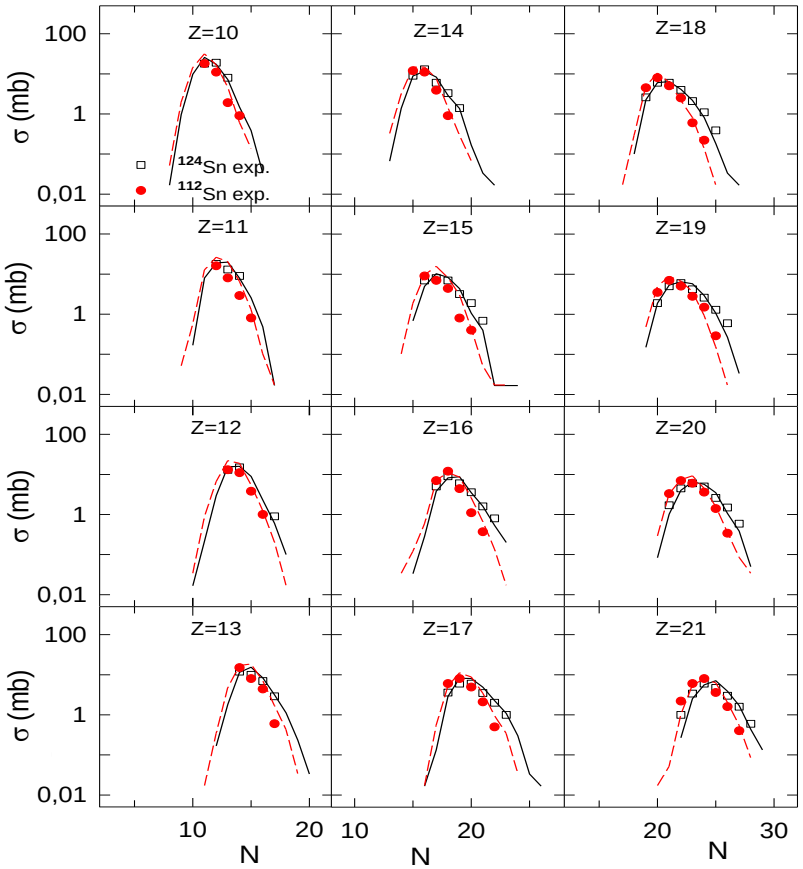

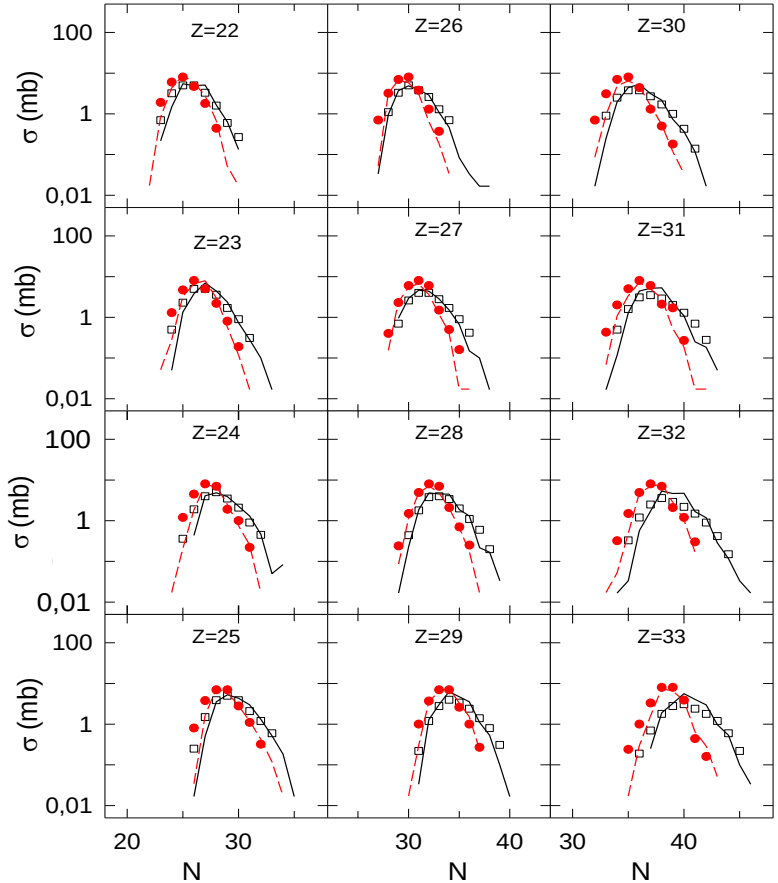

Fig.4.a-b. Isotopic cross-sections of measured fragments in reactions ^{112}Sn + ^{112}Sn (solid red dots), and in ^{124}Sn + ^{124}Sn (open squares) for the final fragments from Z=10 to Z=46.

In order to obtain the best fit with experimental data, we observe that values of symmetry energy γ increases with increasing mass of the sources As.

Z charge intervals	112Sn γ (MeV)	124Sn γ (MeV)
Z=10-17	16	16
Z=18-25	19	18
Z=26-31	21	20
Z=32-37	23	19
Z=38-45	25	18

Isotopic distributions of final fragments from Z=10 to Z=46

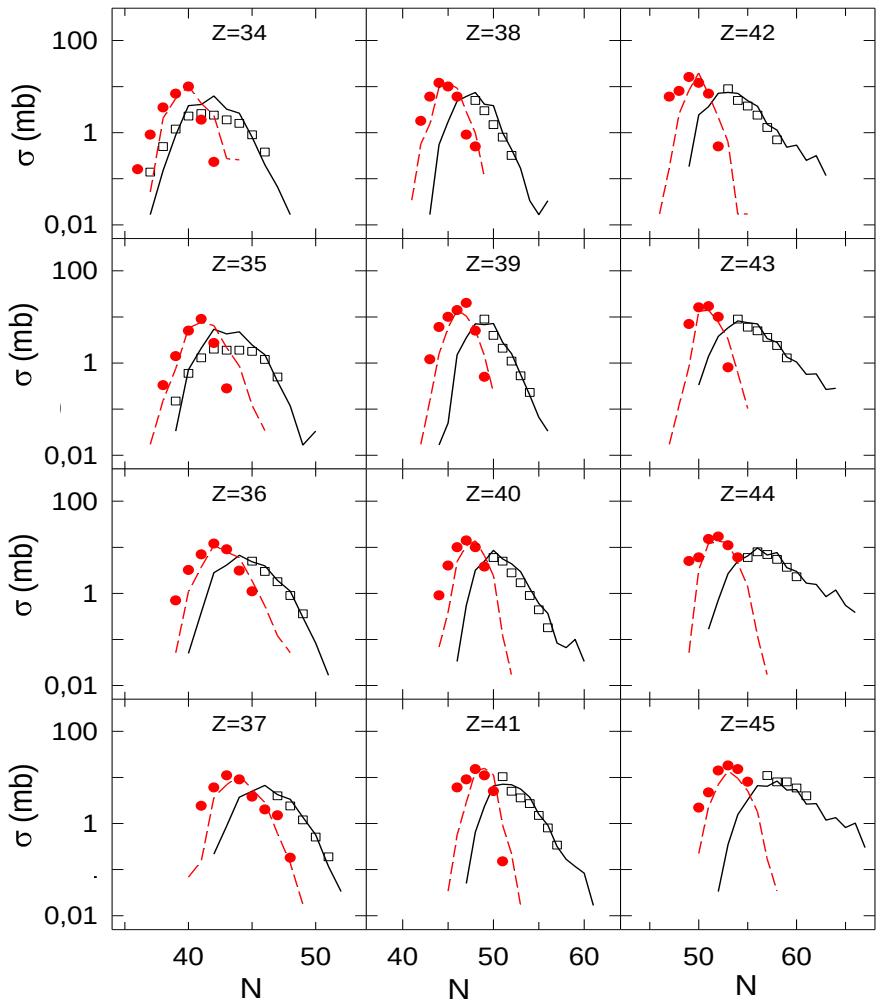

Fig.4 c. Isotopic distributions in the charge interval Z= 34-45

Z charge intervals	112Sn γ (MeV)	124Sn γ (MeV)
Z=10-17	16	16
Z=18-25	19	18
Z=26-31	21	20
Z=32-37	23	19
Z=38-45	25	18

The Main Conclusions for FRS Analysis

It is confirmed that a significant reduction of γ is found necessary to reproduce the isotopic distributions. This is in agreement with our previous results obtained for ALADIN data.

Neutron rich sides of isotopic curves are much more sensitive to γ, this sensitivity is larger for ^{124}Sn for large fragments. By this reason, isotopic curves of the fragments with the same Z for the both projectiles can be reproduced by different values of the symmetry energy parameter γ . Therefore, the symmetry energy of fragments should be important especially for the nuclear species close to the neutron dripline.

Similar neutron-rich nuclei may exist in stellar matter, during the collapse of massive stars and in neutron stars. They are also important for nucleosynthesis as seed nuclei.

Reactions at Fermi Energy Region: MSU-Experiments

We have theoretically investigated isospin dependence in peripheral asymmetric $^{112}Sn + ^{124}Sn$ and $^{124}Sn + ^{112}Sn$ reaction systems at 50 MeV/nucleon projectile energy at National Superconducting Cyclotron of MSU.

Isotopic yield, N/Z and isoscaling observables for light particles were analyzed. We calculate the primary (hot) and secondary (cold) fragment distributions and isotopic yields emitted from quasiprojectile sources assumed to be formed in two reaction systems 112Sn + 124Sn and 124Sn + 112Sn as follows:

A0 = 91, Z0 = 40 (with N/Z = 1.275) for $^{112}Sn + ^{124}Sn$ (N/Z=1.24 for ^{112}Sn)

A0 = 98, Z0 = 40 (with N/Z = 1.450) for $^{124}Sn + ^{112}Sn$ (N/Z=1.48 for ^{124}Sn)

at Ex = 5 MeV/nucleon of excitation energy. These two sources have the same proton number but different N/Z ratio (isospin) as the combined systems, respectively.

Isoscaling in Nuclar Multifragmentation

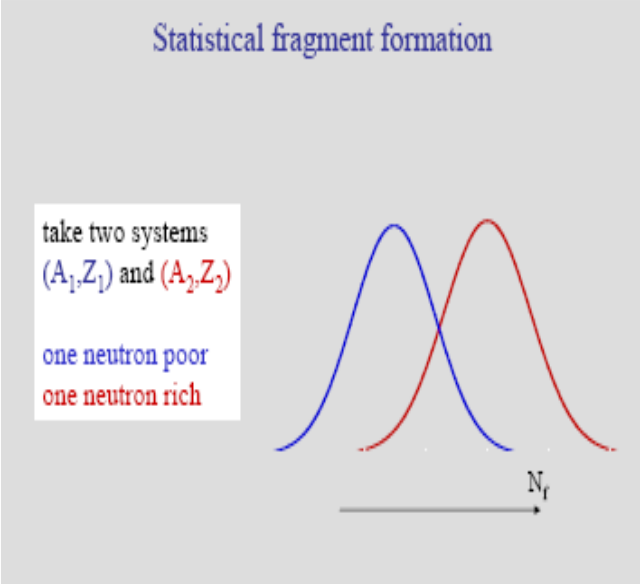

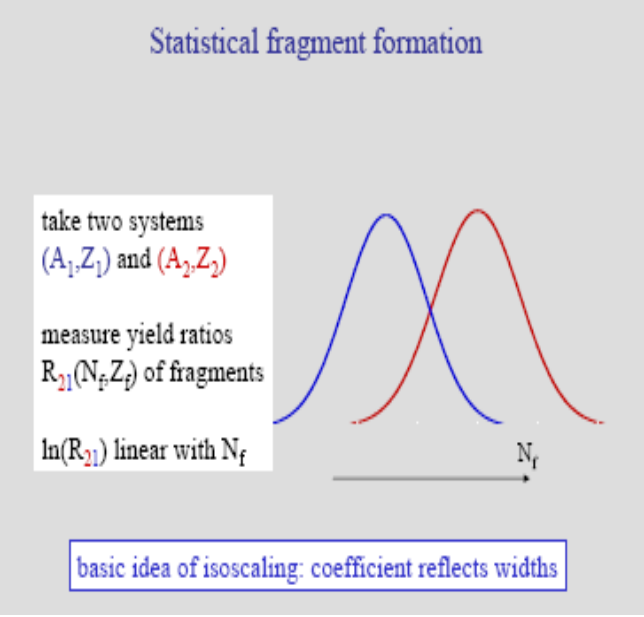

Isoscaling has been observed over a variety of reactions including evaporation, strongly damped binary collision, and nuclear multifragmentation.

It is seen that ratios of isotope yields emitted from two reactions exhibit an exponential dependence on the neutron and proton number of the isotope. Let Y_2 denotes the yield of neutron reach and Y_1 denotes the yield of neutron poor elements. Then the isoscaling ratio is defined as follows:

$$R_{21} = \frac{Y_2(N,Z)}{Y_1(N,Z)} = C\exp(\alpha N + \beta Z)$$

where $R_{21}(N,Z)$ is known as the isoscaling ratio, and the $Y_2(N,Z)$ denotes the yield of the fragments of neutron rich element while $Y_1(N,Z)$ denotes the yield of the fragments of neutron poor element. Here C, α and β are fitting parameters. Experimentally and theoretically approximated formula:

$$\alpha T \approx -4\gamma\,(Z_1^2/A_1^2 - Z_2^2/A_2^2)$$

T is known, then symmetry energy coefficient γ can be obtained by using the obtained isoscaling coefficient α.

Isoscaling in Nuclear Multifragmentation

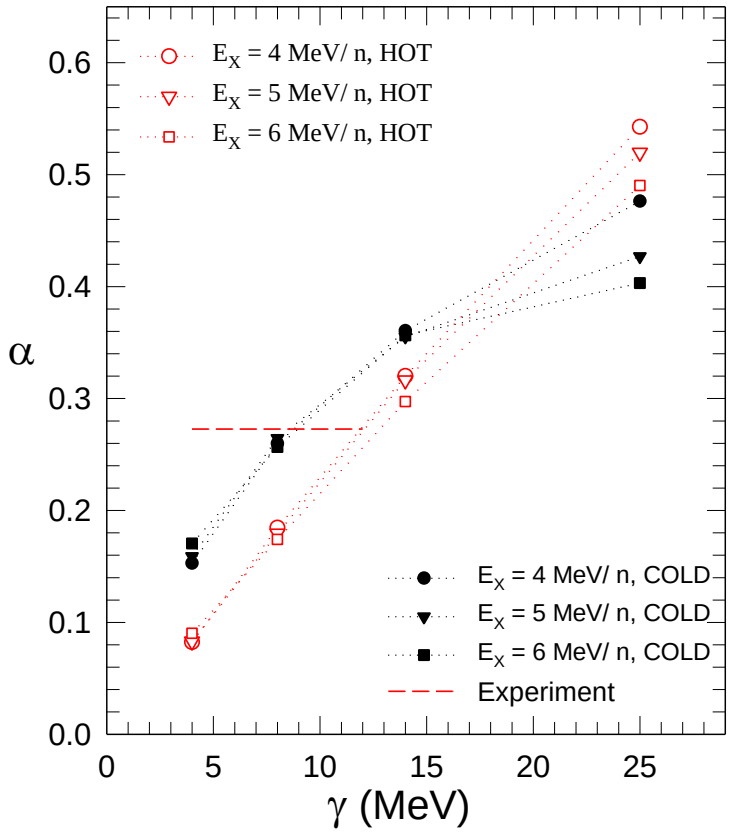

Fig.1.Predicted values of isosscaling parameter α from Eq. (1) for the two diff sources formed in $^{112}Sn+^{124}Sn$ and $^{124}Sn+^{112}Sn$ reactions.

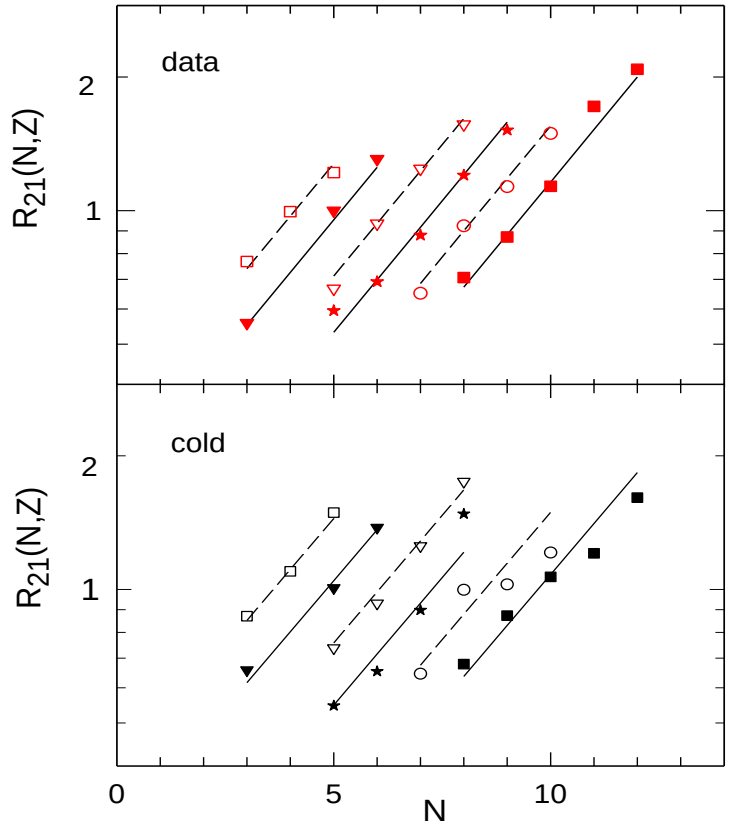

Fig.2.Upper panel for exp data, lower for SMM prediction at γ ~14 MeV.

Exp data: α_{exp} = 0.262 and Theory: α_{final} = 0.254 optimized at intersection, γ ~14 MeV.

Lines representing best fits of the predicted R_{12} ratios to eq.(1), linear and parallel reflected by a single constant isoscaling parameters α_{hot} = 0.262. Space represents increase of R_{12} equal space from single constant value of β= -0.28.

Isoscaling analysis provides very good agreement with the data at reduced γ values.

Isoscaling in Nuclar Multifragmentation

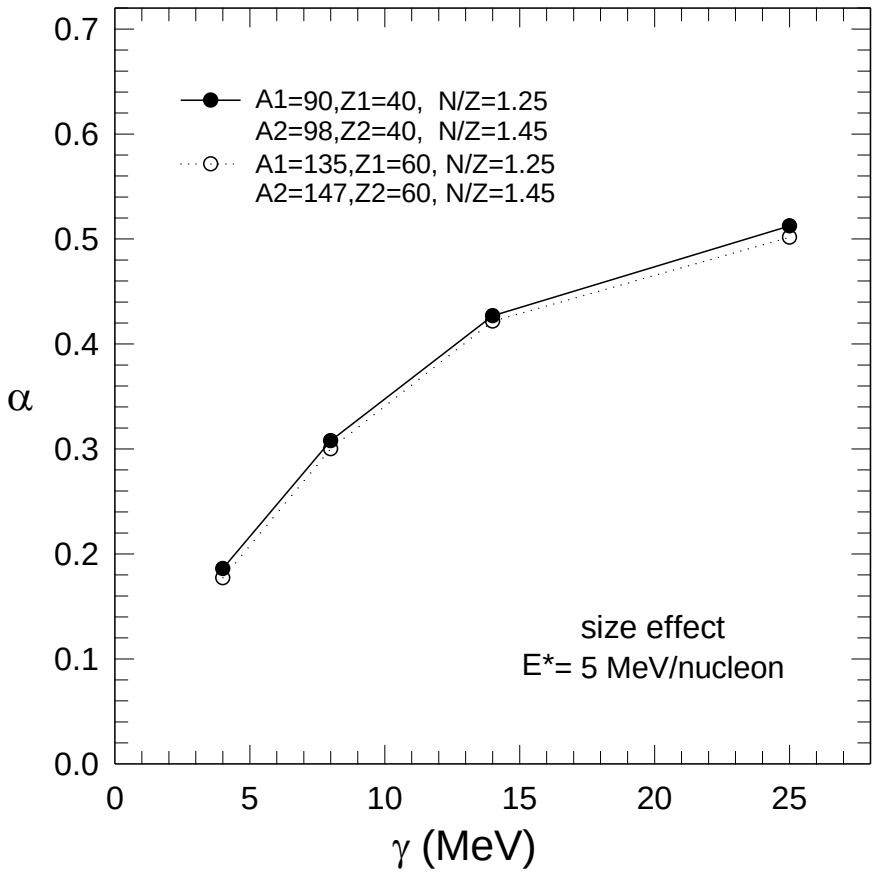

Volume effect on isoscaling parameters is negligible. But N/Z values strongly influence.

Fig.3. The values of isoscaling coefficients α calculated from Eq. (3) as a function of symmetry-term coefficent γ at E_* = 5 MeV/nucleon, for two different pairs of sources: (A1 =9 0,Z1 = 40), (A2 = 98,Z2 = 40) denoted by solid lines with closed symbols, and (A1 = 135,Z1 = 60), (A2 = 147,Z2 = 60) denoted by dotted lines with open symbols, at 50 % size difference, with equal N/Z ratios.

The Main Conclusions for MSU experiments

We have demonstrated that modified variations of N/Z difference (neutron enrichment) of the sources strongly influence the isoscaling parameter α, and hence the extracted values of symmetry-term coefficient γ for hot fragments, while the effect of the size of the sources can be negligible.

The results indicated that the nucleon exchange between the target and projectile nuclei must be considered in order to reproduce the experimental data.

This is in agreement with our previous analyses of ALADIN and FRS data at relativistic energies (600 MeV/n and 1 GeV/n respectively).

We have no more data for MSU experiments at ermi energy regime for heavier fragments to make a comparison with FRS results for near projectile fragments. However, we have FAZIA data newly published:

Ref. S. Piantelli et al., Phys. Rev. C 103, (2021) 014603.

FAZIA-Experiments

FAZIA Collaboration (Four pi A and Z Identification Array),

at Fermi energies E/A = 35 MeV/A, Kr^{80} beams on $Ca^{40,48}$ targets, isotopic composition of QP residue in the charge range Z=19-24, and its decay products were measured at at the Superconducting Cyclotron of the Laboratori Nazionali del Sud (LNS) of INFN, Catania.

Simulations & Calculations with Statistical Ensemble Approach for the reactions:

$Kr^{80} + Ca^{48}$

$Kr^{80} + Ca^{40}$

Experimental and theoretically predicted results for isotope distribution were compared.

Ref. [1} S. Piantelli et al., Phys. Rev. C 103, (2021) 014603. Experiment (FAZIA)

Ref. [2] R. Ogul, A.S. Botvina, …, W. Trautmann, Phys. Rev. C 107, (2023) 054606. Theory

FAZIA experiments

We have studied the isotopic yields of nuclei produced in peripheral collisions of 80Kr + 40,48Ca at 35 MeV/nucleon within the statistical multifragmentation model (SMM) and compare it with the FAZIA data.

The fragments emitted from the projectile sources are successfully described with the previously established ensemble method.

The results indicated that the nucleon (isospin) exchange between the target and projectile nuclei seems inevitable in order to reproduce the experimental data. This is obtained in the isotopic contents of the fragments produced in both reaction systems with neutron rich Ca-48 and neutron poor Ca-40 targets.

In the both reaction simulations the N/Z ratios of Kr projectile sources (PS) are corresponding to the number of neutrons transferred from one nucleus to the another. It was verified by a slightly higher N/Z=1.25 value of PS than that of the projectile 80Kr (N/Z=1.22) when the target is neutron rich Ca-48 , and a slightly lower N/Z=1.17 value in case of neutron poor Ca-40 target.

FAZIA experiments

In the both reaction simulations the N/Z ratios of Kr projectile sources (PS) are corresponding to the number of neutrons transferred from one nucleus to the another. It was verified by a slightly higher N/Z=1.25 value of PS than that of the projectile 80Kr (N/Z=1.22) when the target is neutron rich Ca-48 , and a slightly lower N/Z=1.17 value in case of neutron poor Ca-40 target. Optimized values of the symmetry energy parameters are in consistent with our FRS analysis. Due to Ar-40(Z=18) pollution, Z>18 is taken as lower limit for QP residue to exclude the pollution.

Z charge range	Ca-40 γ (MeV)	Ca-48 γ (MeV)
Z=19,20	**19**	**18**
Z=21,22	**20**	**19**
Z=23,24	**21**	**20**

As a novel development we have also introduced a midrapidity low-density $\rho = (1/6)\rho 0$ source which can be responsible for the so-called neck-like fragment emission.

Isotope Distributions for Z=19-24:FAZIA-data & theory

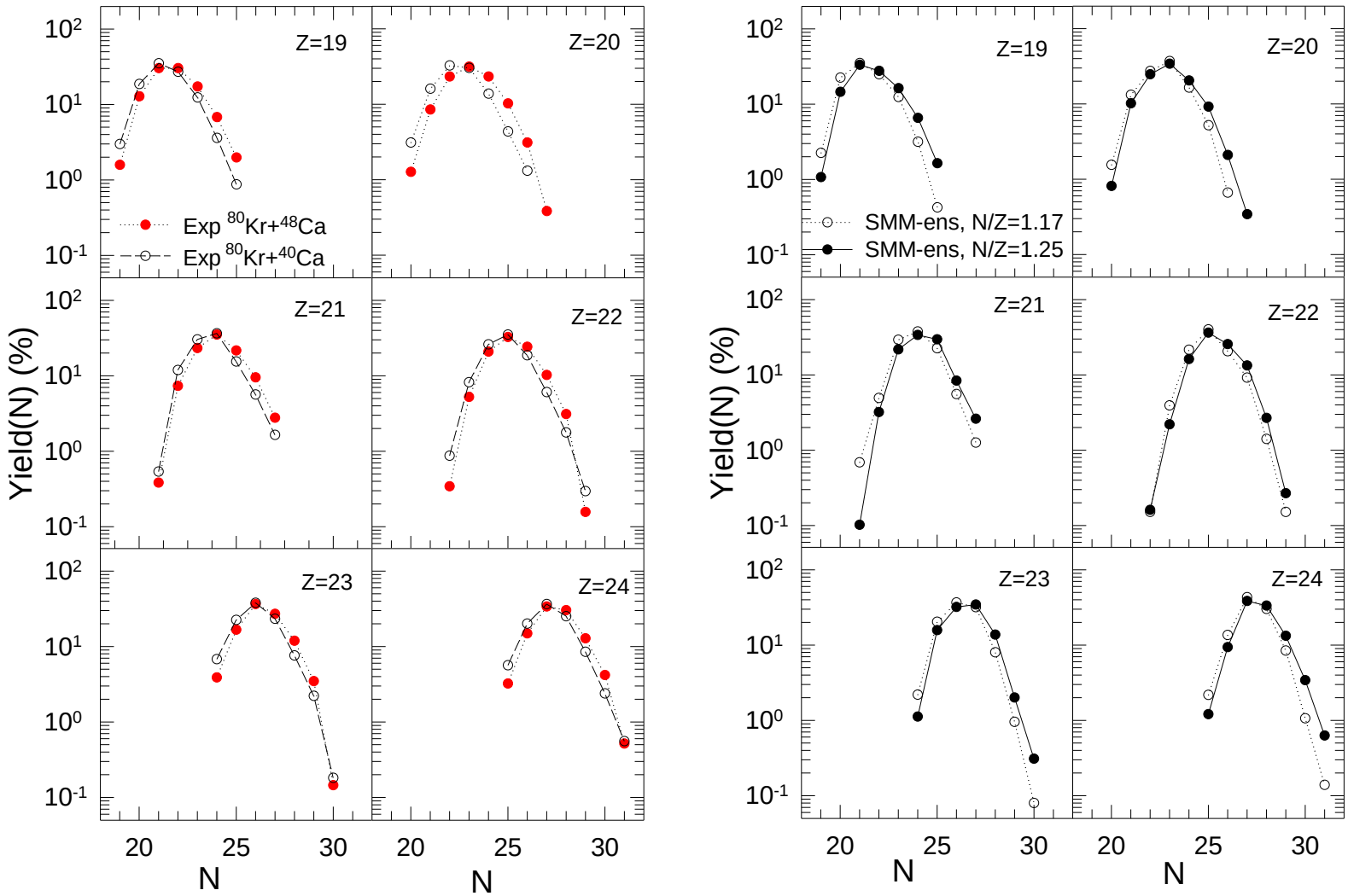

Fig.1: Left panel show experimental results for neutron rich Ca-48 and neutron-poor Ca-40 targets (FAZIA data: Ref.[1]. Right panel shows the theoretical predictions for both reaction systems.

ısotope distributions: FAZIA-data (PRC 103,2021)&Theory

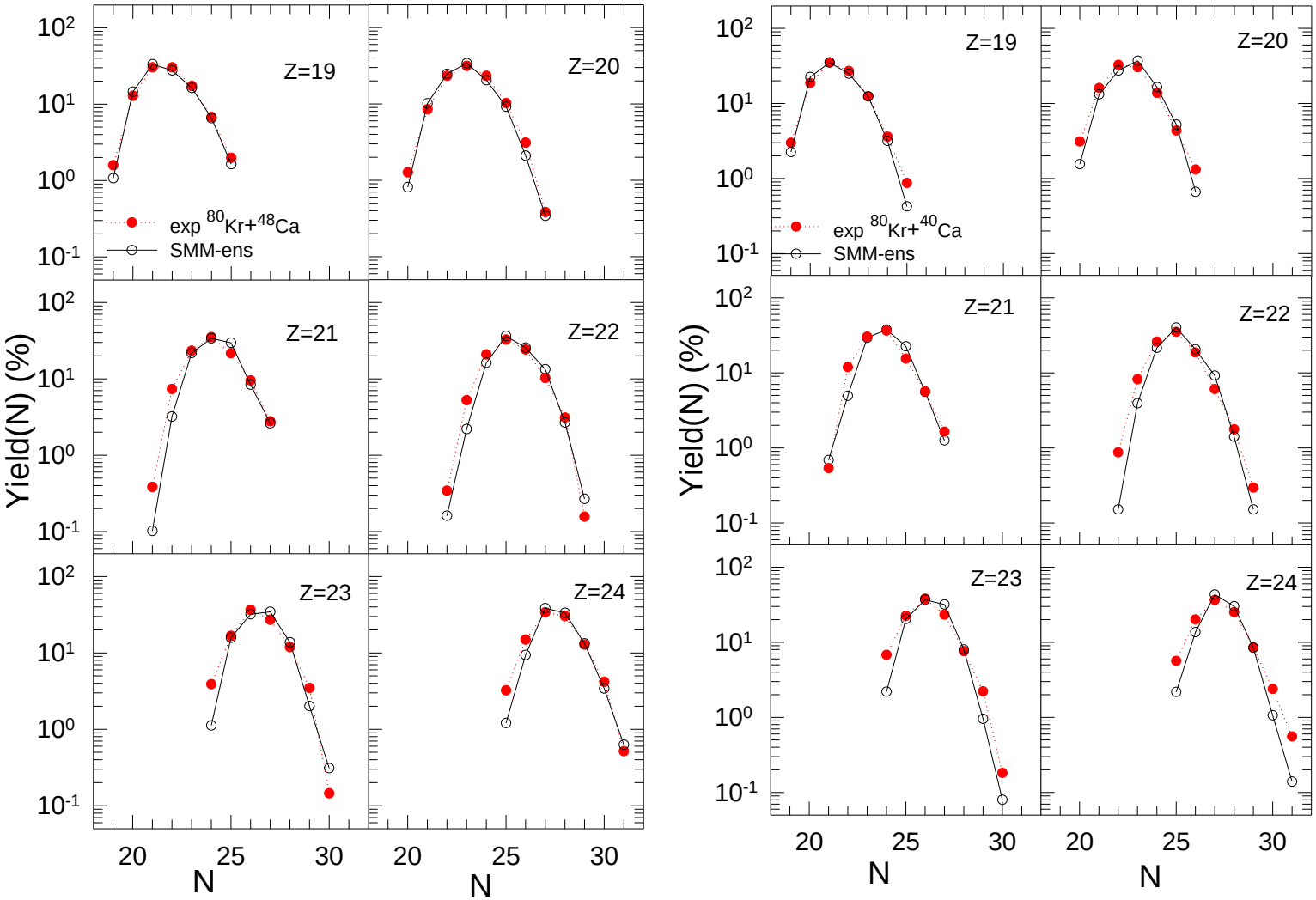

Fig.2:. Red solid circles shows experimental, data and empty circles show the prediction of SMM. The values of optimized ymmetry energy coefficients γ were given in the table.

Relative Yields of Light Particles: Fazia Data & Theory

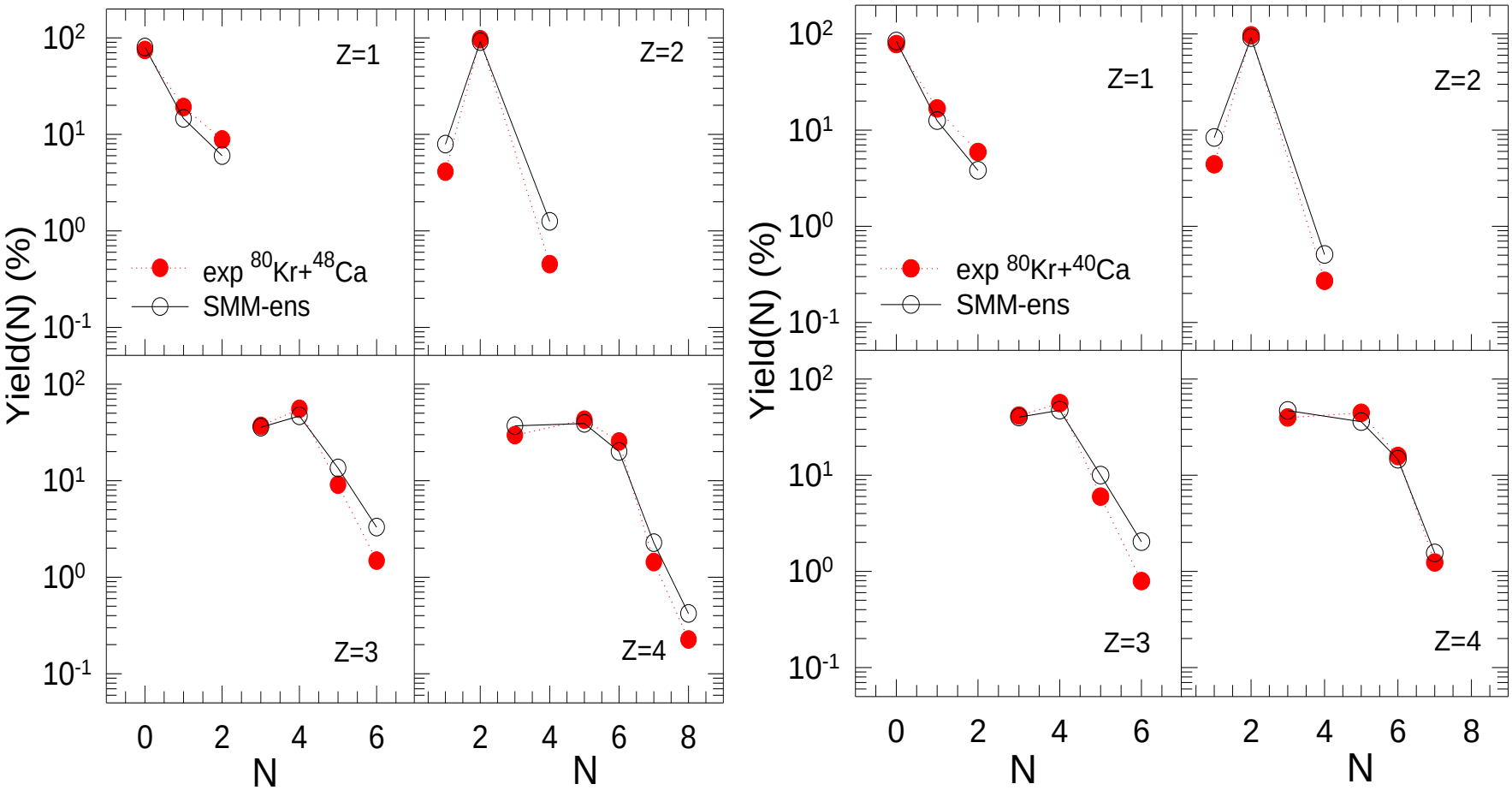

Fig 3: Predicted isotope distributions for Z = 1-4 fragments for ^{84}Kr+^{48}Ca (left panels) and ^{80}Kr+^{40}Ca (right panels) and the stars to the FAZIA data [1]. Good agreement with FRS results with the same γ values.

Average N/Z values of Light Particles: Fazia Data & Theory

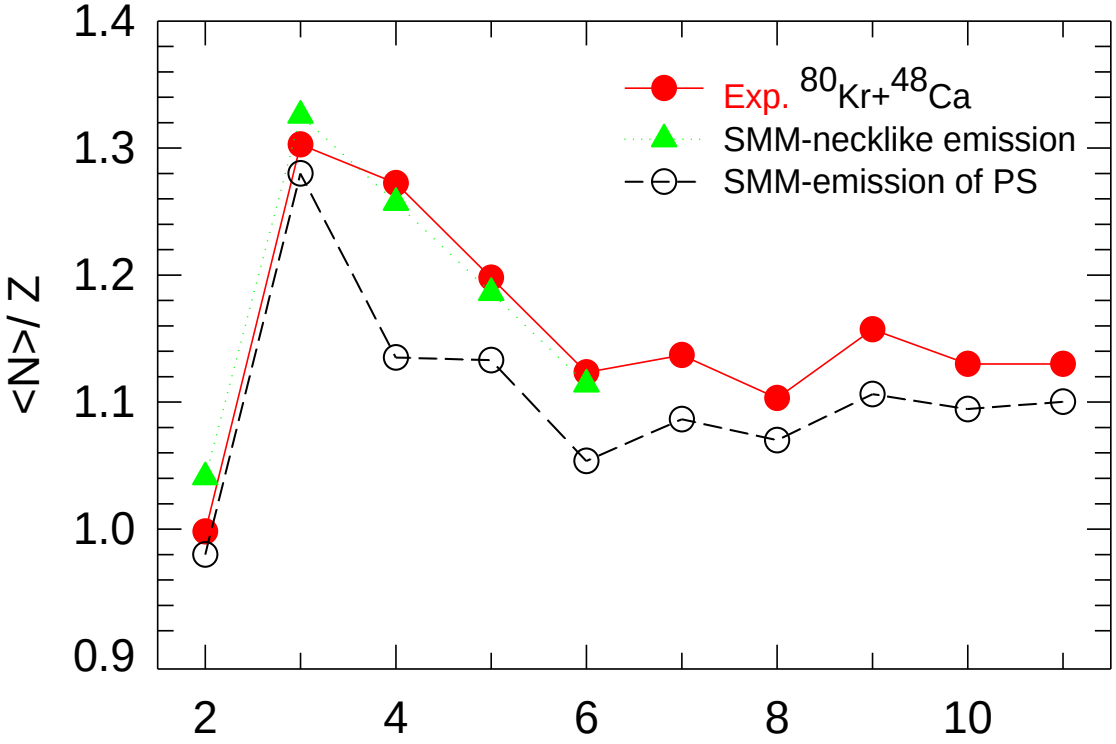

Fig. 4. Comparison of experimental and theoretical average N/Z values of the midrapidity fragments as a function of their charge number Z, for the 80Kr + 48Ca reaction. Solid red circles are for the experimental midrapidity fragments defined as backward emitted with respect to the projectile rest frame (Ref. [1]). The triangles are for the results of SMM calculations of the decay of the midrapidity source. for the source with A=19, Z=8 (i.e., N/Z=1.375), at the excitation energy of 5 MeV/nucleon, the freeze-out density ρ=ρ0/6, and the reduced symmetry energy term γ=14 MeV. The empty circles are for the SMM decay of the PS.

CONCLUSIONS

The experimental data, consequently, is reproduced by decreasing symmetry energy parameter to the lower values than $\gamma < 25$ MeV at low density freze-out.

We reproduce the experimentally observed isotope production at Fermi energy regime and relativistic energies that shows the universality of the limitation of the excitation energy stored at residual sources.

If the projectile velocity is in the range of Fermi velocity nucleon exchange is İnevitable. At relativistic energies, however, Fermi spheres of projectile and target are well separated, and nucleon exchange is very unlikely.

Similar justifications were also shown by various facilities with the analyses of the experiments including Miniball/Miniwall (MSU), Multics (INFN), INDRA (GANIL), CHIMERA (LNS), NIMROD, MARS, FAUST (TAMU), LASSA, ISiS (IUCF), FASA (JINR), ALADIN, FRS (GSI), EOS (LBNL) and so on. For all simulations, the key theoretical point is to obtain the most adequate selection of the equilibrium state of the excited sources.

CONCLUSIONS

Extracted information from the analyses of experiments will be particularly useful for the studies of exotic nuclei far from stability and for the simulation of astrophysical events such as supernova explosion and the crust of neutron stars.

Also, binding energy of hypernuclei can be related to the production of the hypernuclei. Binding energy can be calcuated from the yields of hypernuclei products by using double-ratios (see Ref.).

This may allow to understand the hyperon-nucleon (YN), hyperon-hyperon (YY) and many body aspects of three-flavor interactions (i.e., including u, d, and s quarks) and to study dynamical change of the nuclear structure. Further studies ongoing in the facilities including: STAR, ALICE, HypHI collab, PANDA,CBM, Super-FRS, RB3 at FAIR, BM@N, MPD at NICA, HIAF-China, JPARC-Japan, etc.

Ref: N. Buyukcizmeci, at al., **Phys. Rev. C 98** (2018) 064603; **EPJA** (2019) 55.

Thank you.